A Linearized Implicit Scheme for Solving Logarithmic Nonlinear Schrödinger's Equation

Abstract

In this research, we will develop a numerical scheme for solving the nonlinear logarithmic Schrödinger's equation using the Linearized implicit scheme, that has second-order accuracy in space and time, with significant savings in computational time. We then compare the results to those obtained previously using the Crank-Nicolson scheme of the finite difference method. The stability and precision of this method will be evaluated before it is implemented. Precise solution and conserved quantities will be used to prove the efficiency as well as reliability of the method that has been proposed. Additionally, tests are conducted to explore the interactions that take place between two and three solitons. The numerical findings of our investigation demonstrated that the behavior of interactions is elastic.

Keywords

linearized implicit scheme; exact solutions; stability; bounded domain; one soliton; gaussons; soliton interaction.

1 Introduction

The applications of the non-linear Schrödinger's (NLS) equation are extensive and varied, spanning fields as diverse as nonlinear optics, biomathematics, plasma physics and fluid dynamics. Recent years have seen a surge in interest in the dynamics of solitons in optical signals as one of the most important areas of nonlinear optical research [1]-[17]. Since the beginning of the century, researchers have paid more attention to optical solitons exhibiting log-law nonlinearity, also referred as optical Gaussons. Multiple analytical results are already published [17]. Integrability is a subject that is receiving a lot of attention from researchers throughout the world. Most of these nonlinear forms make the NLS equation inherently unintegrable. Log-law nonlinearity is one type of nonlinear dynamics. The explosion of the logarithmic nonlinearity creates challenges in developing numerical techniques and establishing error bounds for the logarithmic nonlinear Schrödinger's (log NLS) equation. Logarithmic Schrödinger's equation across unbounded sectors is incredibly difficult to numerically solve due to the non-linear nature of the phenomena and the lack of clear boundaries in the domain [18].

In 2000, Biswas and Aceves introduced a perturbation technique for the analysis of optical solitons. These solitons are characterized by a perturbed nonlinear Schrödinger's equation [1]. In 2008, Biswas analyzed the effects of perturbation terms on optical soliton cooling [2]. In the same year, Kohl et al. investigated nonlinearities such as power law, parabolic law, dual-power law, and Kerr law [3]. An exact one-soliton solution to Schrödinger's equation with a log-law nonlinearity in the presence of unsteady disturbances was obtained by Biswas et al. in 2010 [4]. In 2010, Khalique and Biswas came up with a way to integrate the Schrödinger's equation with log-law nonlinearity into a single equation. In order to do this, the Lie symmetry method was employed. It was therefore possible to identify the stationary solutions [5]. Biswas and Milovic described the one soliton solution of Schrödinger's equation exhibiting log law nonlinearity. This was accomplished by using the solitary wave approach [6]. In a study conducted by Biswas et al. in 2011, it was described how Schrödinger's nonlinear equation, that also governs optical solitons, operates by utilizing non-Kerr law nonlinearity in the existence of perturbation components with complete nonlinearity. This study was conducted in order to investigate the existence of perturbation elements with comprehensive non-linearity [7]. In 2012, Biswas et al. reported about the soliton solution for non-linear optics using variational principle [8]. For the logarithmic Schrödinger's equation in any dimension and with non-radial perturbations, Alex showed in 2016 that the ground state is orbitally stable [19]. In 2016, Troy provided evidence that all feasible solutions to the logarithmic Schrödinger problem involve a positive ground condition [20]. To analyze the logarithmic Schrödinger equation, Hongwei Zhang and Qingying introduced a family of potential wells and utilized the fractional logarithmic Sobolev inequality in 2017 [21]. Standing waves with a peak-Gausson profile were analyzed for a nonlinear logarithmic Schrödinger's equation with -interaction by Jaime and Nataliia in 2017 [22].

Bao et al. (2019) performed an analysis on two numerical approaches for solving the logarithmic Schrödinger's equation (LogSE), which consisted of a regularized splitting method and a regularized conservative Crank–Nicolson finite difference method (CNFD) [23]. In 2019, Hongwei et al. paid special attention to the approximation solution of the log NLS equation issue in unbounded domains. Given its nonlinearity and unboundedness, the logarithmic Schrödinger's equation is difficult to numerically solve on unbounded domains [18]. An error bound for a regularized finite difference method was developed and obtained by BAO et al. (2019) for the log NLS equation. Error bounding and numerical method development for the log NLS equation are both complicated by the explosion of logarithmic nonlinearity [24]. In 2019, Wazwaz conducted research on the logarithmic Schrödinger's equation by employing the variation iteration method, analyzing it in both cases where a detuning term was present and when it was not [25]. Bandpass filters and multi-photon absorption were also topics that Salman and colleagues addressed in the same year. In addition to this, he provided an explanation for the mean free velocity of optical Gaussons that moved with stochastic disturbance [26]. The Laplace-Adomian decomposition method is a methodology that can be effective in the investigation of optical Gaussons, as stated by Gaxiola et al. in the year 2020. To prevent a numerical blow-up in the regularized space-fractional logarithmic Schrödinger problem, Bianru and enhua studied the spectral technique of regularized Lie-Trotter splitting in 2021 [27]. The detuning term was included in some

of the numerical simulations as well as omitted in others. In addition to that, the error analysis of the scheme was discussed [17]. Three new logarithmic nonlinear amplitude equations were presented by Darvishiat et al. in 2022. The purpose of this research was to identify the origins of the Gaussian solitary waves generated by these logarithmic equations [28].

The physical behavior of equations can be understood by applying numerical methods. As a result, in our research we will address the linear implicit scheme for solving the nonlinear logarithmic Schrödinger's equation, which is used in this equation for the first time, to the researchers' knowledge.

2 Problem Statement

In this work, the nonlinear logarithmic Schrödinger's equation will be solved numerically, using a second-order linear implicit differential technique.

$$i\frac{\partial u}{\partial t} + a\frac{\partial^2 u}{\partial x^2} + b\log\left(|u|^2\right)u = 0\ , \tag{1}$$
$$i{=}\sqrt{-\mathbf{1}},\ (x_L \le x \le x_R,\ 0 \le t \le T),$$

the initial and boundary conditions:

$$u(x,0) = g(x),\ x_L \le x \le x_R,$$
$$u(x_L,t) = 0 = u(x_R,t),\ 0 \le t \le T,$$

where a denotes the group velocity dispersion coefficient and b denotes the nonlinear term coefficient [6]., and in order to avoid complicated calculation, we assume

$$u(x,t) = v(x,t) + iw(x,t), \tag{2}$$

where $v(x,t)$ and $w(x,t)$ are the real functions. When we substitute (2) into (1), we get the coupled system below:

$$\frac{\partial v}{\partial t} + a\frac{\partial^2 w}{\partial x^2} + b\log(|u|^2)w = 0, \tag{3}$$
$$\frac{\partial w}{\partial t} - a\frac{\partial^2 v}{\partial x^2} - b\log(|u|^2)v = 0. \tag{4}$$

Exact soliton solution to the log NLS equation is given by [6],[8] ,[17], [26], [29], [30] and [31]

$$u(x,t) = Ae^{-B^2(x-st)^2}e^{i(-kx+\zeta t+\theta)}, \tag{5}$$

where $s = -2ak$, $B = \sqrt{b/2a}$, $\zeta = 2b\log(A) - ak^2 - b$, and $ab > 0$.
The amplitude of Gaussons is denoted by A, while the center of the Gausson's phase is represented by θ. The phase component wave number is ζ, s is the frequency-related Gausson velocity. and B is the inverse width.

In the log NLS equation (1), the three conserved values are [6],[26],[29] and [31]

$$I_1 = \int_{-\infty}^{\infty} |u|^2\, dx, \tag{6}$$

$$I_2 = i\int_{-\infty}^{\infty} [u^* u_x - u u_x^*]dx, \tag{7}$$

$$I_3 = \int_{-\infty}^{\infty} [a\,|u_x|^2 - b\,|u|^2\log|u|^2 + b\,|u|^2]dx, \tag{8}$$

where u^* denote the complex conjugate of u.

3 Numerical Method

To develop a numerical scheme for resolving the system denoted by Eqs. (3) and (4), the region $R = (x_L \leq x \leq x_R)\mathrm{x}(t > 0)$ with boundaries defined by the parameters $x = x_L, x_R$ and the axis $t = 0$ is covered by a rectangular mesh of points with coordinates, $x = x_m = x_L + mh$, $m = 0, 1, 2, ..., N$, $t = t_n = nk$, $n = 0, 1, 2, ...$, $h = \frac{x_R - x_L}{N}$, Where h and k denote the respective space and time increments. We make the assumption that $v(x_m, t_n)$, $w(x_m, t_n)$ are the exact solutions at the point (x_m, t_n), and $V(x_m, t_n)$, $W(x_m, t_n)$ are approximation of the exact solutions. The linearized implicit approach for solving $(3) - (4)$ is provided by

$$\frac{V_m^{n+1} - V_m^{n-1}}{2k} + \frac{a}{h^2}\delta_x^2[\frac{W_m^{n+1} + W_m^{n-1}}{2}] + bz_m^n[\frac{W_m^{n+1} + W_m^{n-1}}{2}] = 0, \tag{9}$$

$$\frac{W_m^{n+1} - W_m^{n-1}}{2k} - \frac{a}{h^2}\delta_x^2[\frac{V_m^{n+1} + V_m^{n-1}}{2}] - bz_m^n[\frac{V_m^{n+1} + V_m^{n-1}}{2}] = 0, \tag{10}$$

where

$$z = \log(|u|^2),$$

Eqs. (9) and (10) may be written as follows:

$$V_m^{n+1} - V_m^{n-1} + \frac{ak}{h^2}\delta_x^2[W_m^{n+1} + W_m^{n-1}] + bkz_m^n[W_m^{n+1} + W_m^{n-1}] = 0, \tag{11}$$

$$W_m^{n+1} - W_m^{n-1} - \frac{ak}{h^2}\delta_x^2[V_m^{n+1} + V_m^{n-1}] - bkz_m^n[V_m^{n+1} + V_m^{n-1}] = 0, \tag{12}$$

by expanding the operators in (11) and (12) we possible get

$$\begin{aligned} & V_m^{n+1} + r_1(W_{m-1}^{n+1} - 2W_m^{n+1} + W_{m+1}^{n+1}) + r_2 z_m^n W_m^{n+1} \\ = \; & V_m^{n-1} - r_1(W_{m-1}^{n-1} - 2W_m^{n-1} + W_{m+1}^{n-1}) - r_2 z_m^n W_m^{n-1}, \end{aligned} \tag{13}$$

and

$$\begin{aligned} & W_m^{n+1} - r_1(V_{m-1}^{n+1} - 2V_m^{n+1} + V_{m+1}^{n+1}) - r_2 z_m^n V_m^{n+1} \\ = \; & W_m^{n-1} + r_1(V_{m-1}^{n-1} - 2V_m^{n-1} + V_{m+1}^{n-1}) + r_2 z_m^n V_m^{n-1}, \end{aligned} \tag{14}$$

where

$$r_1 = \frac{ak}{h^2},\ r_2 = bk,\ m = 1, 2, ..., N-1.$$

The system represented by Eqs. (13) and (14) is a three-level scheme that is implicitly linear U^{n+1}, U^n, U^{n-1} in unknown U^{n+1}, this system can be expressed as a matrix vector as follows:

$$M\mathbf{U}^{n+1} = \mathbf{F}(\mathbf{U}^{n-1}, \mathbf{U}^n) \tag{15}$$

Where $\mathrm{U}= [V, W]^t$ and M is a tridiagonal block matrix

$$M(u) = \begin{bmatrix} A_1 & C_1 & 0 & \cdots & 0 \\ B_2 & A_2 & C_2 & \ddots & \vdots \\ 0 & \ddots & \ddots & \ddots & 0 \\ \vdots & \ddots & B_{n-1} & A_{n-1} & C_{n-1} \\ 0 & \cdots & 0 & B_n & A_n \end{bmatrix}.$$

And the following components of the matrix M may be described in detail:

$$B_m = \begin{bmatrix} 0 & r_1 \\ -r_1 & 0 \end{bmatrix}_m,\ A_m = \begin{bmatrix} 1 & a_{12} \\ a_{21} & 1 \end{bmatrix}_m,\ C_m = \begin{bmatrix} 0 & r_1 \\ -r_1 & 0 \end{bmatrix}_m,$$

where

$$\begin{aligned} a_{12} &= -2r_1 + r_2 z_m^n, \\ a_{21} &= 2r_1 - r_2 z_m^n, \\ m &= 1, 2, ..., N. \end{aligned}$$

The system in Eq. (15) may be solved using Crout's method.To begin, two preliminary conditions are required: one at $t = 0, U^0$ which can be derived from the initial condition, and the other at $t = k, U^1$ which can be obtained from any two-level scheme or the precise solution.

3.1 Accuracy of the scheme

To investigate the correctness of the suggested method, we investigate the accuracy of (9), and we substitute the numerical solution V_m^n, W_m^n by the exact solution v_m^n, w_m^n, and the following expansions may be produced by utilizing Taylor's series expansion of all terms in equation (9), round the point (x_m, t_n),

$$\begin{aligned} \frac{v_m^{n+1} - v_m^{n-1}}{2k} &= \frac{\partial v}{\partial t} + \frac{k^2}{6}\frac{\partial^3 v}{\partial t^3} + ..., \\ \frac{1}{2h^2}\delta_x^2(w_m^{n+1} + w_m^{n-1}) &= \frac{\partial^2 w}{\partial x^2} + \frac{h^2}{12}\frac{\partial^4 w}{\partial x^4} + \frac{k^2}{2}\frac{\partial^4 w}{\partial x^2 \partial t^2} + ..., \\ z_m^n\left(\frac{W_m^{n+1} + W_m^{n-1}}{2}\right) &= zW + \frac{k^2}{2} z \frac{\partial^2 W}{\partial t^2} + ..., \end{aligned} \tag{16}$$

Now, if we replace Eqs. (16) with Eq. (9), we get

$$\begin{aligned} LTE &= [\frac{\partial v}{\partial t} + a\frac{\partial^2 w}{\partial x^2} + bzw] + \frac{k^2}{2}\frac{\partial^2}{\partial t^2}(\frac{1}{3}\frac{\partial v}{\partial t} + a\frac{\partial^2 w}{\partial x^2} \\ &\quad + bzw) + a\frac{h^2}{12}\frac{\partial^4 w}{\partial x^4} + ..., \end{aligned} \tag{17}$$

using differential Eq (3) the first bracket is equal to zero and hence

$$LTE = \frac{k^2}{2}\frac{\partial^2}{\partial t^2}[\frac{1}{3}\frac{\partial v}{\partial t} + a\frac{\partial^2 w}{\partial x^2} + bzw] + a\frac{h^2}{12}\frac{\partial^4 w}{\partial x^4} + ..., \tag{18}$$

Eq. (18) represents a local truncation mistake. The method is second-order in time and second-order in space. The accuracy of scheme (10) may be studied in the same manner.

3.2 Stability of the scheme

To examine the numerical method's stability, we can observe that the scheme in (1) is nonlinear, and the van-Neumann stability can only be used for linear schemes. We can make the scheme linear by freezing all the terms that make it not linear.

$$i(\mathbf{U}_m^{n+1} - \mathbf{U}_m^{n-1}) + r\delta_x^2(\mathbf{U}_m^{n+1} + \mathbf{U}_m^{n-1}) + kb\lambda(\mathbf{U}_m^{n+1} + \mathbf{U}_m^{n-1}) = 0, \tag{19}$$

Where

$$r = a\frac{k}{h^2}, \quad \lambda = \max(\log|u|^2)$$

To apply the von Neumann stability analysis to Eq. (19), we assume

$$\mathbf{U}_m^n = e^{\alpha nk} e^{i\beta mh}, \quad \delta_x^2 \mathbf{U}_m^n = -4\sin^2(\frac{\beta h}{2})\mathbf{U}_m^n \tag{20}$$

Table 1: First test: (a) error analysis; compare the linearized implicit scheme and the Crank-Nicolson method.

$h = 0.1$, $k = 0.0001$				
time	$L - M$		$C - N$	
	$\mathrm{L}_\infty(V)$	$\mathrm{L}_\infty(W)$	$\mathrm{L}_\infty(V)$	$\mathrm{L}_\infty(W)$
0.00	0.000000	0.000000	0.000000	0.000000
1.00	0.000833	0.001875	0.000833	0.001875
2.00	0.001345	0.001596	0.001344	0.001595
3.00	0.002503	0.003055	0.002503	0.003054
4.00	0.002845	0.003668	0.002844	0.003667
5.00	0.004200	0.003933	0.004200	0.003933

When we plug Eqs. (20) into Eq. (19) we obtain

$$i(e^{\alpha k} - e^{-\alpha k}) - 4r\sin^2(\frac{\beta h}{2})(e^{\alpha k} + e^{-\alpha k}) + kb\lambda(e^{\alpha k} + e^{-\alpha k}) = 0,$$

and it's also possible to write it as

$$e^{\alpha k}(i - \gamma + kb\lambda) = e^{-\alpha k}(i + \gamma - kb\lambda), \tag{21}$$

where

$$\gamma = 4r\sin^2(\frac{\beta h}{2})$$

It's possible to write Eq. (21) like this:

$$e^{2\alpha k} = \frac{[i + (\gamma - kb\lambda)]}{[i - (\gamma - kb\lambda)]} \tag{22}$$

It is simple to see from equation (22), that $\left|e^{\alpha k}\right| = 1$, and as a result, we are able to state that the scheme is unconditionally stable in accordance with the von Neumann stability analysis.

3.3 Numerical tests

In this section, we will perform several experiments to evaluate the performance of the current method and compare our results with those of the Crank-Nicholson method [31]. With the addition of some new tests, now we will look at the following issues:

3.3.1 Single Soliton

For the sake of applying the precise solution in equation (6), we set the starting condition at $t = 0$, $u(x, 0) = Ae^{-B^2x^2}e^{i(-kx+\theta)}$, in the first test, the following criteria are taken into consideration:
$h = 0.1$, $k = 0.0001$, $s = 0.4$, $A = 0.4$, $a = 0.5, b = 1$, $\theta = 0.5$, $x_L = -4$, $x_R = 6$.
In order to investigate the correctness of the suggested technique, we calculate the $\mathrm{L}_\infty-$ error norm, which is defined by

$$L_\infty = \|U^n - u^n\|_\infty = \max|U(x_m, t_m) - u(x_m, t_m)|$$

In the second test, the following criteria are taken into consideration:

$$\begin{aligned} h &= 0.05,\ k = 0.001,\ s = 0.4,\ A = 0.4,\ a = 0.5, \\ b &= 1,\ \theta = 0.5,\ x_L = -4,\ x_R = 8 \end{aligned}$$

Table 2: First test: (b) quantities preserved compare of the Linearized implicit scheme and Crank Nicolson method

$h = 0.1,\ k = 0.0001$						
time	$L - M$			$C - N$		
	I_1	I_2	I_3	I_1	I_2	I_3
0.00	0.200530	-0.159582	0.783269	0.200530	-0.159582	0.783269
1.00	0.200530	-0.159572	0.783249	0.200530	-0.159571	0.783248
2.00	0.200530	-0.159579	0.783265	0.200530	-0.159579	0.783266
3.00	0.200530	-0.159573	0.783251	0.200530	-0.159572	0.783251
4.00	0.200530	-0.159577	0.783259	0.200530	-0.159578	0.783260
5.00	0.200530	-0.159577	0.783257	0.200530	-0.159577	0.783257

Table 3: Second test error Analysis and quantities Preserved using Linearisation method

$h = 0.05,\ k = 0.001$					
time	$L_\infty(V)$	$L_\infty(W)$	I_1	I_2	I_3
0.00	0.000000	0.000000	0.200530	-0.160213	0.784259
2.00	0.000342	0.000402	0.200530	-0.160213	0.784258
4.00	0.000722	0.000929	0.200530	-0.160213	0.784258
6.00	0.001286	0.000984	0.200530	-0.160213	0.784258
8.00	0.001822	0.001498	0.200530	-0.160213	0.784257
10.00	0.001739	0.002074	0.200530	-0.160213	0.784257

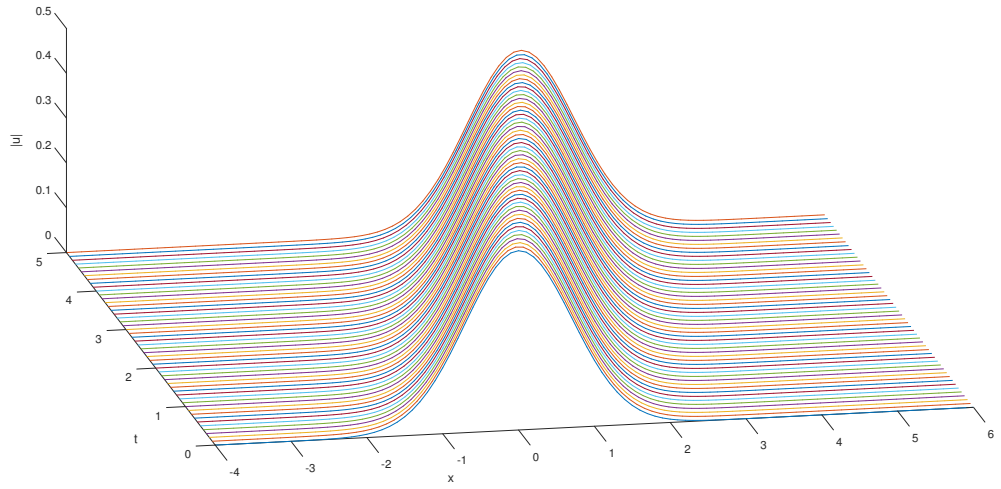

Figure 1: Simulation of single soliton using Linearization implicit scheme with parameters $h = 0.1, k = 0.0001, s = 0.4, 0 \leq t \leq 5$

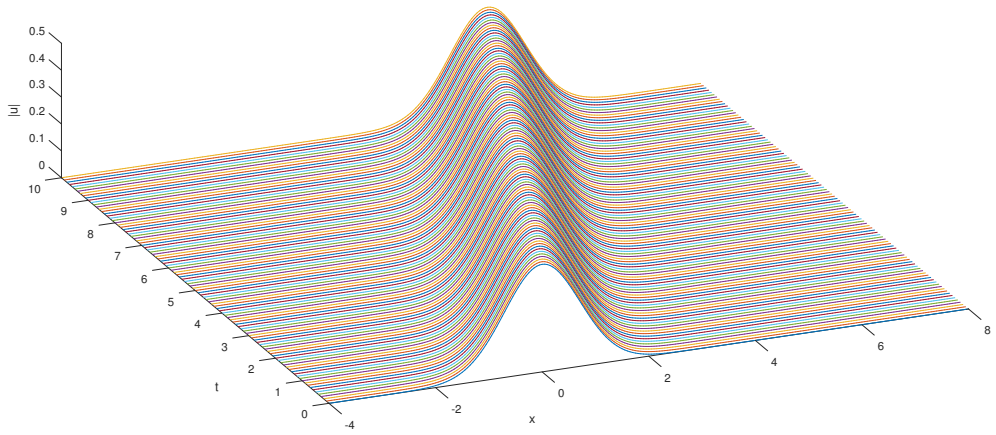

Figure 2: Simulation of single soliton using Linearization implicit scheme with parameters $h = 0.05, k = 0.001, s = 0.4, 0 \leq t \leq 10$

In table 1, there is a comparison of the error analysis of the linearized implicit scheme and the Crank-Nicolson method employing L_∞ norms, respectively. Table 2 shows the conserved quantities of one soliton using the linearized implicit scheme and the Crank-Nicolson method, respectively. By looking at the two tables, it is clear that the linear implicit scheme gives accurate results that are identical to a large extent with the Crank-Nicolson method for the preserved quantities of soliton by using the same parameters, and the accuracy of the linearized implicit increases as h becomes smaller, as we can see in Table 3. Figure 1 shows a single soliton solution obtained using the linearized implicit scheme with parameters h=0.1, k=0.0001, and s=0.4. Figure 2 shows a single soliton solution obtained using the linearized implicit scheme with parameters h=0.05, k=0.001, and s=0.4.

3.3.2 Collision of two solitons

When we do a second numerical experiment, we look at how two solitons interact together. We use the following form to do that.

$$u(x,t) = A \sum_{m=1}^{q} \exp[-B^2(x - x_m - s_m t)^2] \exp(i(-k_m(x - x_m) + \zeta_m t + \theta)),$$

$$s_m = -2ak_m,\ B = \sqrt{b/2a}, \zeta_m = 2b\log(A) - ak_m^2 - b,\ q = 2\ and\ ab > 0,$$

In the third test, the following criteria are taken into consideration:

$$\begin{aligned} h &= 0.1,\ k = 0.0001,\ s_1 = 0.8,\ s_2 = -0.4,\ A = 0.4,\ a = 0.5, \\ b &= 1,\ \theta = 0.5,\ x_1 = 0,\ x_2 = 4.5,\ x_L = -4,\ x_R = 10 \end{aligned}$$

Table 4: Third test: quantities preserved compare of two solitons interaction of the Linearized implicit scheme and Crank Nicolson method

$h = 0.1,\ k = 0.0001$						
time	$L - M$			$C - N$		
	I_1	I_2	I_3	I_1	I_2	I_3
0.00	0.401069	-0.159233	1.613564	0.401069	-0.159233	1.613564
1.00	0.401069	-0.159125	1.613448	0.401069	-0.159125	1.613450
2.00	0.401068	-0.159250	1.613313	0.401069	-0.158250	1.613315
3.00	0.401069	-0.157636	1.610116	0.401068	-0.157637	1.610117
4.00	0.401069	-0.158954	1.613604	0.401068	-0.158945	1.613603
5.00	0.401069	-0.158669	1.611677	0.401068	-0.158667	1.611674

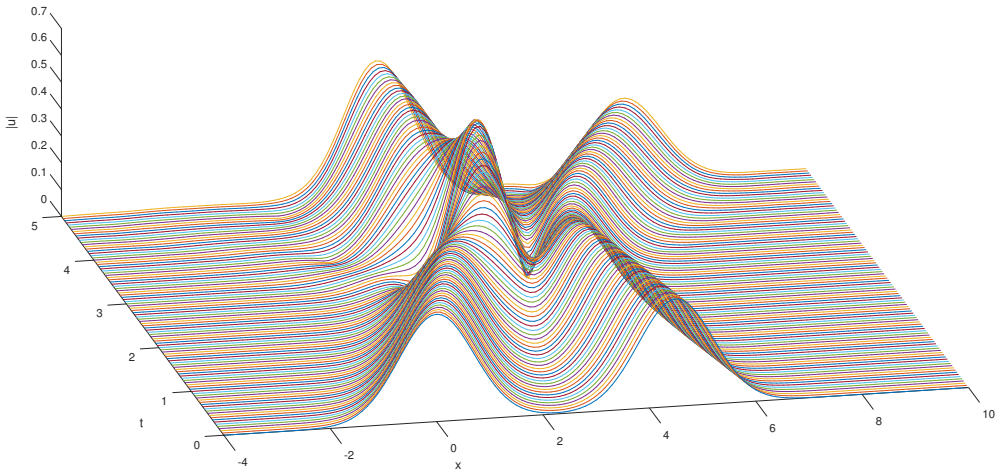

Figure 3: Collision of two solitons using Linearization implicit scheme with parameters $h = 0.1, k = 0.0001, x_1 = 0, x_2 = 4.5, at\ 0 \leq t \leq 5$

Table 3: Comparison of a numerical simulation of the linearized implicit scheme and the Crank-Nicholson method for the collision of two solitons traveling in opposite directions at different speeds from left to right. The speeds are 0.8 and -0.4. It is noted that the two solitons return to their previous form after the collision, as shown in Figure 3.

3.3.3 Interaction of Three Solitons

We use the following form to do that.

$$u(x,t) = A \sum_{m=1}^{q} \exp[-B^2(x - x_m - s_m t)^2] \exp(i(-k_m(x - x_m) + \zeta_m t + \theta)),$$

In the fourth test, the following criteria are taken into consideration:

$$\begin{aligned} h &= 0.1,\ k = 0.0001,\ s_1 = 2.4 = -s_3,\ s_2 = 0.1,\ q = 3,\ A = 0.4,\ a = 0.5, \\ b &= 1,\ \theta = 0.5,\ x_1 = -7,\ x_2 = 0,\ x_3 = 7,\ x_L = -15,\ x_R = 15 \end{aligned}$$

Table 5: Fourth test conserved quantities of three solitons interaction by Linearization implicit scheme

$h = 0.1,\ k = 0.0001$			
time	I_1	I_2	I_3
0.00	0.601591	-0.039906	3.414252
1.00	0.601591	-0.039904	3.412848
2.00	0.601592	-0.040613	3.410579
3.00	0.601592	-0.040668	3.397667
4.00	0.601592	-0.043239	3.411051
5.00	0.601592	-0.042279	3.413648

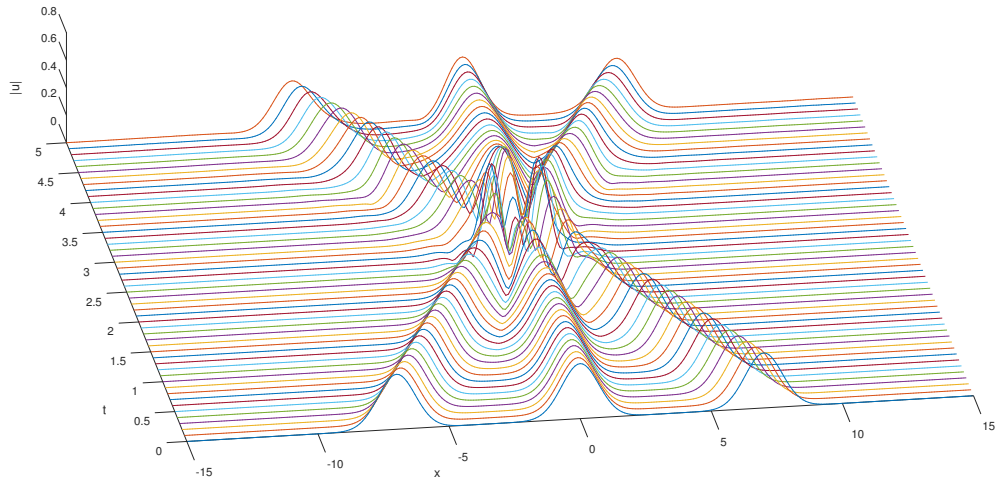

Figure 4: Collision of three solitons using Linearization implicit scheme with parameters $h = 0.1, k = 0.0001, x_1 = -7, x_2 = 0, x_3 = 7 at\ 0 \leq t \leq 5$

Table 5: A numerical simulation of the linearized implicit scheme for the collision of three slithons traveling in opposite directions at different speeds from left to right. The speeds are 2.4, 0.1, and -2.4. It is noted that the solitones return to their previous form after the collision, as shown in Figure 4.

4 Conclusion

For this study, we used the linearization approach to numerically examine the log NLS equation. When comparing the linearization strategy to the Crank-Nicolson method, we discovered that the linearization approach produced nearly as precise results while still preserving the conserved values. The linearization scheme has the same uncondistional stability as the Crank-Nicolson method and is accurate to the second order in space and time. Furthermore, the interaction of two and three solitons with one another is demonstrated. In this case, we observed that the collision between the two and three-solitons were able to maintain the flexibility.

5 Declarations

5.1 Conflict of Interest

The authors state that they have no conflicts of interest to disclose in relation to the current study.

5.2 Data Availability

The article contains the supporting data for the study's findings.

References

[1] BISWAS A., ACEVES A.B., Dynamics of solitons in optical fibers, Journal of Modern Optics 48(7), 2001, pp. 1135–1150.

[2] BISWAS A., MILOVIC D., MAJID F., KOHL R., Optical soliton cooling in a saturable law media, Journal of Electromagnetic Waves and Applications 22(13), 2008, pp. 1735–1746.

[3] BISWAS A., FESSAK M., JOHNSON S., BEATRICE S., MILOVIC D., JOVANOSKI Z., KOHL R., MAJID F., Optical soliton perturbation in non-Kerr law media: Traveling wave solution, Optics and Laser Technology 44(1), 2012, pp. 263–268.

[4] BISWAS A., CLEARY C., WATSON J.E., JR., MILOVIC D., Optical soliton perturbation with time-dependent coefficients in a log law media, Applied Mathematics and Computation 217(6), 2010, pp. 2891–2894.

[5] KHALIQUE C.M., BISWAS A., Gaussian soliton solution to nonlinear Schrödinger equation with log-law nonlinearity, International Journal of Physical Sciences 5(3), 2010, pp. 280–282.

[6] BISWAS A., MILOVIC D., Optical solitons with log law nonlinearity, Communications in Nonlinear Science and Numerical Simulation 15(12), 2010, pp. 3763–3767.

[7] BISWAS A., TOPKARA E., JOHNSON S., ZERRAD E., KONAR S., Quasi-stationary optical solitons in non-Kerr law media with full nonlinearity, Journal of Nonlinear Optical Physics and Materials 20(3), 2011, pp. 309–325.

[8] BISWAS A., MILOVIC D., KOHL R., Optical soliton perturbation in a log-law medium with full nonlinearity by He's semi-inverse variational principle, Inverse Problems in Science and Engineering 20(2), 2012, pp. 227–232.

[9] GREEN P.D., MILOVIC D., LOTT D.A., BISWAS A., Optical solitons with higher order dispersion by semi-inverse variational principle, Progress in Electromagnetics Research 102, 2010, pp. 337–350.

[10] KOHL R., BISWAS A., MILOVIC D., ZERRADE., Optical soliton perturbation in a non-Kerr law media, Optics and Laser Technology 40(4), 2008, pp. 647–662.

[11] WEN-JUN LIU, BO TIAN, TAO XU, KUN SUN, YAN JIANG, Bright and dark solitons in the normal dispersion regime of inhomogeneous optical fibers: Soliton interaction and soliton control, Annals of Physics 325(8), 2010, pp. 1633–1643.

[12] SARMA A.K., Solitary wave solutions of higher-order NLSE with Raman and self-steepening effect in a cubic-quitic–septic medium, Communications in Nonlinear Science and Numerical Simulation 14(8), 2009, pp. 3215–3219.

[13] ZAI-YUN ZHANG, ZHEN-HAI LIU, XIU-JIN MIAO, YUE-ZHONG CHEN, New exact solutions to the perturbed nonlinear Schrödinger's equation with Kerr law nonlinearity, Applied Mathematics and Computation 216(10), 2010, pp. 3064–3072.

[14] ZAI-YUN ZHANG, ZHEN-HAI LIU, XIU-JIN MIAO, YUE-ZHONG CHEN, Qualitative analysis and traveling wave solutions for the perturbed nonlinear Schrödinger's equation with Kerr law nonlinearity, Physics Letters A 375(10), 2011, pp. 1275–1280

[15] Arafat, SM Yiasir, et al. "Parametric effects on paraxial nonlinear Schrödinger equation in Kerr media." Chinese Journal of Physics 83 (2023): 361-378.

[16] Arafat, SM Yiasir, et al. "On nonlinear optical solitons of fractional Biswas-Arshed Model with beta derivative." Results in Physics 48 (2023): 106426.

[17] González-Gaxiola, O., Biswas, Anjan and Alzahrani, Abdullah Kamis. "Gaussons: optical solitons with log-law nonlinearity by Laplace–Adomian decomposition method" Open Physics, vol. 18, no. 1, 2020, pp. 182-188.

[18] Hongwei Lia, Xin Zhaoa, Yunxia Hua, Numerical solution of the regularized logarithmic Schrödinger equation on unbounded domains. Applied Numerical Mathematics, 140(2019):91-103.

[19] Hernandez Ardila A. Orbital stability of Gausson solutions to logarithmic Schrödinger equations. arXiv e-prints. 2016 Jul:arXiv-1607.

[20] Troy WC. Uniqueness of positive ground state solutions of the logarithmic Schrödinger equation. Archive for Rational Mechanics and Analysis. 2016 Dec;222(3):1581-600.

[21] Zhang H, Hu Q. Existence of the global solution for fractional logarithmic Schrödinger equation. Computers & Mathematics with Applications. 2018 Jan 1;75(1):161-9.

[22] Angulo Pava J, Goloshchapova N. Stability of standing waves for NLS-log equation with δ-interaction. arXiv e-prints. 2015 Jun:arXiv-1506.

[23] Bao W, Carles R, Su C, Tang Q. Regularized numerical methods for the logarithmic Schrödinger equation. Numerische Mathematik. 2019 Oct;143(2):461-87.

[24] W. Bao, R. Carles, C. Su and Q. Tang, "Error estimates of a regularized finite difference method for the logarithmic Schrödinger equation". SIAM Journal on Numerical Analysis, 57 (2019): 657-680.

[25] Wazwaz AM, El-Tantawy SA. Optical Gaussons for nonlinear logarithmic Schrödinger equations via the variational iteration method. Optik. 2019 Feb 1;180:414-8.

[26] Khan S, Majid FB, Biswas A, Zhou Q, Alfiras M, Moshokoa SP, et al. Stochastic perturbation of optical Gaussons with bandpass filters and multi-photon absorption. Optik. 2019;178:297–300.

[27] Cheng B, Guo Z. Regularized splitting spectral method for space-fractional logarithmic Schrödinger equation. Applied Numerical Mathematics. 2021 Sep 1;167:330-55.

[28] Darvishi MT, Naja M, Akinyemi L, Rezazadeh H. Gaussons of some new nonlinear logarithmic equations. Journal of Nonlinear Optical Physics & Materials. 2022 May 14;2350013:16.

[29] Girgis L., Milovic D., Hayat T., Aldossary O., Biswas A.,Optical soliton perturbation with log law nonlinearity, Optica Applicata, Vol. XLII, No. 3, 2012DOI:10.5277/oa120301.

[30] Guo, Ya-Shan, Wei Li, and Shi-Hai Dong. "Gaussian solitary solution for a class of logarithmic nonlinear Schrödinger equation in (1+ n) dimensions." Results in Physics 44 (2023): 106187.

[31] Al-Harbi, A., Al-Hamdan, W. and Wazzan, L. (2022) Numerical Methods for Solving Logarithmic Nonlinear Schrödinger's Equation. Journal of Applied Mathematics and Physics,10, 3635-3648.